

APPLICATIONS OF SPECTRAL LINES FOR LOW ELECTRON DENSITY PLASMA DIAGNOSTICS

M. Ivković, S. Jovićević, R. Žikić, N. Konjević

Institute of Physics, 11081 Belgrade, P.O.Box 68, Serbia

Abstract. This work comprises an analysis of optical emission spectroscopy (OES) techniques and results of their application for diagnostics of middle and low electron densities (N_e) in low temperature plasmas. The discussion will be limited primarily to the applications of the methods based on the use of: Stark – widths and shifts of non-hydrogenic neutral and singly ionized atom lines, line shape of neutral helium lines with forbidden components and molecular nitrogen band heads intensities. In this study all these techniques are critically evaluated, tested and applied for diagnostics of microwave induced plasma (MIP), low pressure pulsed arcs or capillary discharge.

1. INTRODUCTION

Low and medium electron density plasmas are extensively used in analytical atomic spectroscopy as a light sources for optical emission spectroscopy (OES), plasma processing and in various technologies, such as laser ablation, thin film deposition, creation of different nanostructures and nanocomposite etc. Therefore, the interest for plasma diagnostics is growing, and the need for improvement of old and development of new techniques is a constant task. Due to their non-perturbative nature, high spatial resolution and variety of different methods, the OES techniques are of particular interest.

In this study, the discussion will be limited primarily to the diagnostics of electron density, N_e , in low temperature plasmas using of non-hydrogenic spectral lines. For other plasma parameters measurements and application of hydrogenic spectral lines for N_e diagnostics, more details can be found in several recent review articles and textbooks [1-5] and references cited therein. Within this work techniques based on Stark – widths and shifts of non-hydrogenic ion and atom spectral lines, the overall line shape of helium atom lines with forbidden component and molecular nitrogen band heads intensities are studied. All these techniques are

applied and tested in different plasma sources and their advantages and drawback discussed.

2. EXPERIMENT

In experimental part of this study two different setups were used. One for the investigations of low pressure pulsed capillary discharge and another one for an atmospheric pressure microwave induced plasma studies. The central part around the axis of the pulsed plasma source is imaged 1 : 1 onto the entrance slit of the 1 m monochromator (inverse linear dispersion 0.833 nm/mm) by means of a 1 m focal length focusing mirror. A 30 mm diaphragm placed in front of the focusing mirror ensures that light comes from the narrow cone about the discharge axis. The spectral line profiles are recorded step-by-step with the instrumental half width of 0.017 nm. Signals from the photomultiplier - PMT are led to a digital storage oscilloscope triggered by the signal from the Rogowsky coil. The main current pulse through the discharge tube induces the trigger pulse. In order to obtain better signal-to-noise ratio an averaging of eight signals at each wavelength step is performed. For more details see references [6, 7].

In cases when radiation from the microwave induced plasma sources – MIP was measured, the 1:1 image is projected on the 20 μ m wide slit by use of a 0.5 m focal length focusing mirror. In that case, signal from the PMT was amplified by the picoammperimeter. More details about sample introduction, gas flow control when using different versions MIP sources one can find in [5, 8].

3. RESULTS

In the following section in front of the experimental and/or mathematical testing of the methods, short review of their fundamental characteristics will be presented.

3.1. Neutral and Singly Ionized Non-hydrogenic Atom Lines

The use of Stark widths and shift of ionized non-hydrogenic atom lines for diagnostics of the electron densities lower than 10^{22} m^{-3} is very rare. At these densities Stark widths are small and comparable with widths due to the other broadening mechanisms, so that high-resolution spectroscopic instrumentation has to be used and deconvolution procedures must be applied.

3.1.1. The Width and Shift of the Neutral Atom Lines

The shape of the neutral atom line in quasistatic approximation for ions is described by the following expression [9]:

$$j_{A,R}(x) = \frac{1}{\pi} \cdot \int_0^{\infty} \frac{H(\beta) d\beta}{1 + (x - A^{4/3} \cdot \beta^2)^2} \quad (1)$$

where $H(\beta)$ is ion microfield distribution, and x is described by $x = (\lambda - \lambda_0 - d_e)/w_e$, λ_0 is the central wavelength of the unperturbed line, d_e is the electron shift and w_e is the electron impact half-halfwidth. Examples of neutral atom plasma broadened line shape for Debye shielding parameter $R = 0.8$ and different values of ion broadening parameter A are presented in Figure 1.

From a large number of generated profiles Griem [4] found that total Stark (full widths at half maximum FWHM) - w_t of line profiles could be expressed within the quasistatic ion approximation as a function of w_e , A and R

$$w_t(T_e) \cong 2w_e(T_e) [1 + 1.75 \times 10^{-4} N_e^{1/4} A(T_e) (1 - 0.068 N_e^{1/6} T_e^{-1/2})] 10^{-16} N_e \quad (2)$$

$$d_t(T_e) \cong [d_e(T_e) \pm 2.0 \times 10^{-4} N_e^{1/4} A(T_e) w_e(T_e) (1 - 0.068 N_e^{1/6} T_e^{-1/2})] 10^{-16} N_e \quad (3)$$

$$d_{t1/2}(N_e, T_e) \approx [d_e(T_e) \pm 3.2 \times 10^{-4} N_e^{1/4} A(T_e) w_e(T_e) (1 - 0.068 N_e^{1/6} T_e^{-1/2})] 10^{-16} N_e \quad (4)$$

where w_t , d_t and $d_{t1/2}$ are measured Stark widths and/or shift of the peak line intensity or shift of the halfwidth, respectively, while w_e , d_e and A are theoretical electron impact half-halfwidth, d_e shift and A ion broadening parameter calculated for $N_e = 10^{16} \text{ cm}^{-3}$ and published in Appendix IV of [4].

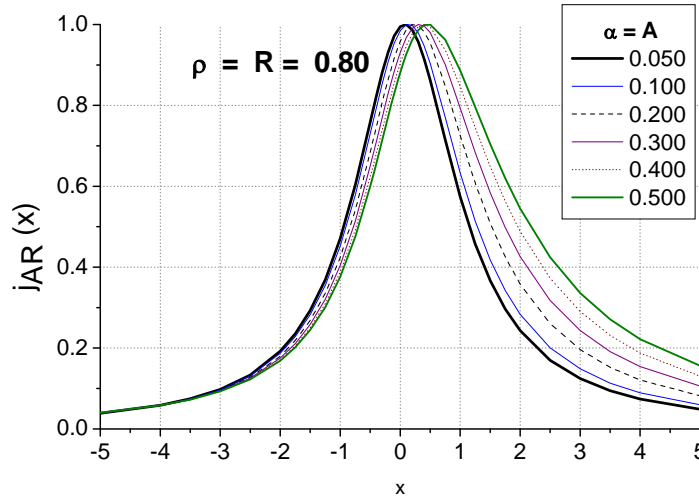


Fig 1. The $j_{A,R}(x)$ profiles of neutral atom lines for $R = 0.8$ and different values of A

It should be noticed that plasma broadened neutral atom lines are asymmetric and that the deconvolution procedure, see e.g. [10,11], differs from symmetric profiles of, for example, ionic lines, see e.g. [12]. Influence of ion dynamics especially in case of light elements such as helium [13,14] is also important and

must be taken in account. For a number of lines correction factors w_{exp}/w_t determined by Konjevic [15] from the comparison of theory and large number of high accuracy experimental data. This enables more precise electron density determination.

This technique was tested in the capillary discharge with gas mixture of 2.4% Ne, 5.6% He and 92 % H₂ at pressure $p = 4$ mbar. The maximum discharge current of $I = 400$ A with $t = 2.7$ μ s was obtained by discharging $C = 0.36$ μ F, charged up to $U = 7$ kV. By use of excitation temperature $T_{\text{exc}} = 33\ 000$ K determined from Boltzmann plot of O II lines, correction factors from [15] and tabulated values of w_e and A [4] the electron density $N_e = (4.8 \pm 0.2) \times 10^{22}$ m⁻³ from the He I : 388.8, 471.3 and 501.6 nm spectral lines was determined. For the determined electron density and w_e value in Appendix IV of [4] for Ne I spectral line at 594.483 nm very good agreement between experimental and generated Voigt profile was obtained. The observed Ne I lines were symmetrical, within the uncertainty of experiment indicating that small ion broadening contribution is small, see Figure 2.

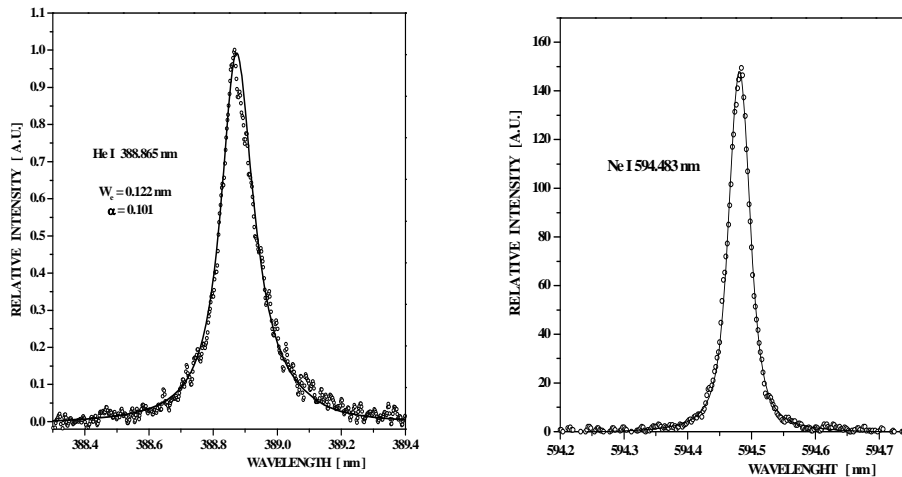


Fig 2. a) The recorded He I 388.865 nm line (\circ) fitted with $j_{\text{AR}}(x)$ theoretical profile with data taken from [4] for $N_e = 5.2 \times 10^{22}$ m⁻³ and $T_e = 33000$ K and b) The recorded Ne I 594.483 nm line (\circ) fitted with Voigt profile for $N_e = 4.8 \times 10^{22}$ m⁻³ and $T_e = 33000$ K.

It should be noticed that from fitted $j_{\text{AR}}(x)$ profile of the He I 388.8 nm line $W_e = 0.122$ nm i.e. $N_e = 5.2 \times 10^{22}$ m⁻³ is obtained, but after applying w_{exp}/w_t correction factor determined in [15] the value of 4.8×10^{22} m⁻³ is determined.

3.1.2. The Comparison of the Theoretical and Experimental Profiles

The another and more accurate way for electron density determination is based on comparison of whole experimental and theoretical line profiles, see example in Fig.2 [16-18]. In order to test the possibility of determining plasma and line parameters by using deconvolution techniques and especially the six fit parameter deconvolution - SFPD procedure [18] from one line profile only (without independent plasma parameters and shift measurements) the theoretical line profiles are generated from Eq.(1). We analyzed theoretical profiles $j_{A,R}(x)$ with the following sets of parameters: 1) various R values ($0 \leq R \leq 0.8$) and largest value of $A = 0.075$ reported in [19]; 2) different pairs of A and R values with fixed electron impact w_e and ion contribution w_i and 3) fixed total Stark widths w_t and R values for various sets of w_e and A.

The Case 1. is illustrated by Fig. 3. The FWHM of these lines for the whole range of R changes from 2.133 to 2.188, i.e. difference is only 0.055 (in x units) while shapes are very similar. This means that for typical w_e values around 0.1 nm at 10^{17} cm^{-3} [19] the difference in half width corresponds to only 0.0055 nm for the whole range of R values. Such a small difference between profiles in a large range of R values raises a question: Is any deconvolution capable of detecting so small differences of line shapes in particular if one is using pulsed plasma source and shot-to-shot technique for line profile recording or study the astrophysical plasmas.

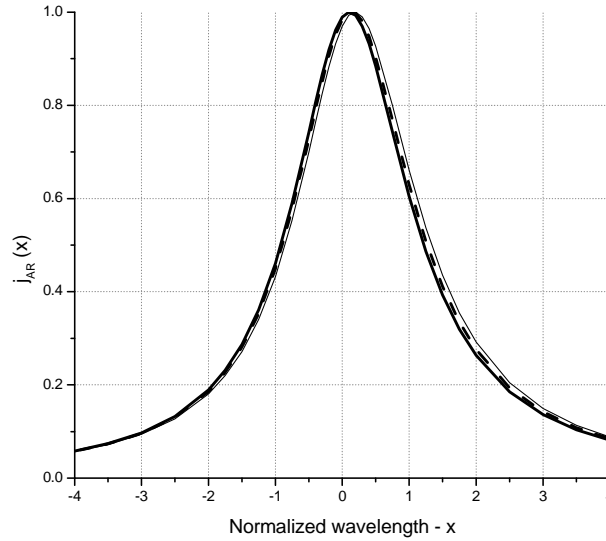


FIGURE 3. The $j_{A,R}(x)$ profiles of neutral atom lines for $w_e = 2$, $d_e = 0$, $A = 0.075$ and different values of: $R = 0$ (thick line), 0.4 (dashed line) and 0.8 (thin line).

In the Case 2., from Eq. (2), after several iterations of this approximate formula many (A,R) pairs with the same electron impact, w_e , and ion contribution, w_i i.e. with the same total Stark width w_t are determined, see several examples in Table 1.

Table 1. Different sets of parameters for the same w_t and total ion shift d_{it} . A_1 - calculated from Eq.(2), A_2 - determined by an iteration process.

w_e	w_t	d_i	R	A_1	A_2
2	2.41	0.47	0.55	0.2	0.2
2	2.41	0.47	0	0.118	0.142
2	2.41	0.47	0.2	0.138	0.162
2	2.41	0.47	0.8	0.294	0.24

The shapes of the lines with parameters given in Table 1 are practically indistinguishable in a typical line profiles presentation. Consequently, the line shape only cannot be used for plasma diagnostics and line parameters determination.

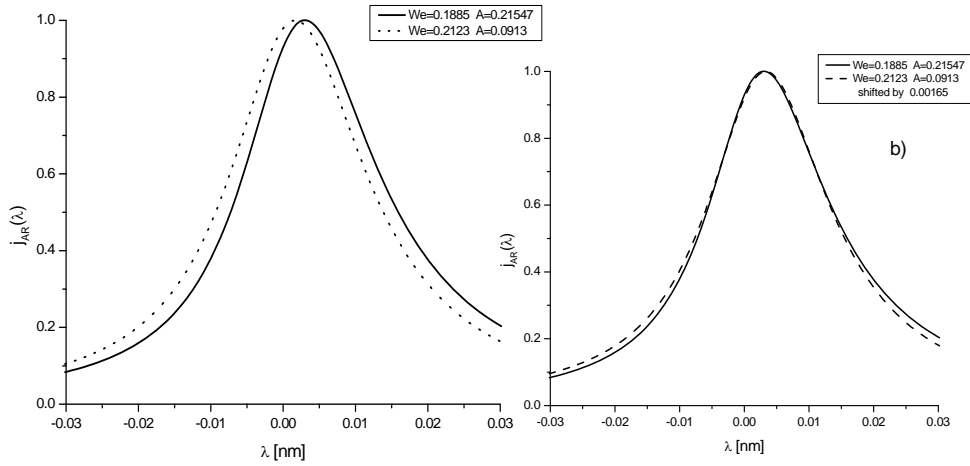


Fig 4. The $j_{A,R}(x)$ profiles for $R = 0.48$ and different values of w_e and A ; $w_e = 0.188$, $A = 0.215$ (solid line); $w_e = 0.212$, $A = 0.091$ (dotted line). a) shifted profiles and b) profiles with the shift normalized to the same value.

In the Case 3, by using Eq.(2), whole set of (w_e, A) pairs for the same value of w_t and R were calculated. In this case profiles are not identical, but they differ slightly at the line wings, see Fig. 4b. These differences are so small that deconvolution of profiles recorded from pulsed sources using shot-to-shot technique in the presence of impurity lines can't distinguish one from another. Figure 4a illustrates the importance of precise shift measurements for determination of N_e in these cases.

The analysis of line profiles is even more complex when all three parameters w_e , A and R are varied. With different combinations of these parameters profiles with exactly the same w_t with very small differences in shape can be obtained.

3.2. Helium lines with Forbidden Component

In the case of helium plasmas, electron density can be determined by using the shape of some visible He I lines with forbidden components. These strong lines, belonging to the $2^3P - n^3D$ series ($n = 4$ for 447.1 nm and $n = 5$ for 402.6 nm) and to the $2^1P - n^1D$ series ($n = 4$ for 492.2 nm), have in plasma forbidden components $2^3P - n^3F$ or $2^1P - n^1F$, respectively. The complex structures of these lines, see Fig.5, are extensively studied both theoretically, by applications of unified, MMM or close coupling (CC) theories, and experimentally. The inclusion of ion dynamic effects in theoretical descriptions of helium lines with forbidden components greatly improves agreement with experimental results.

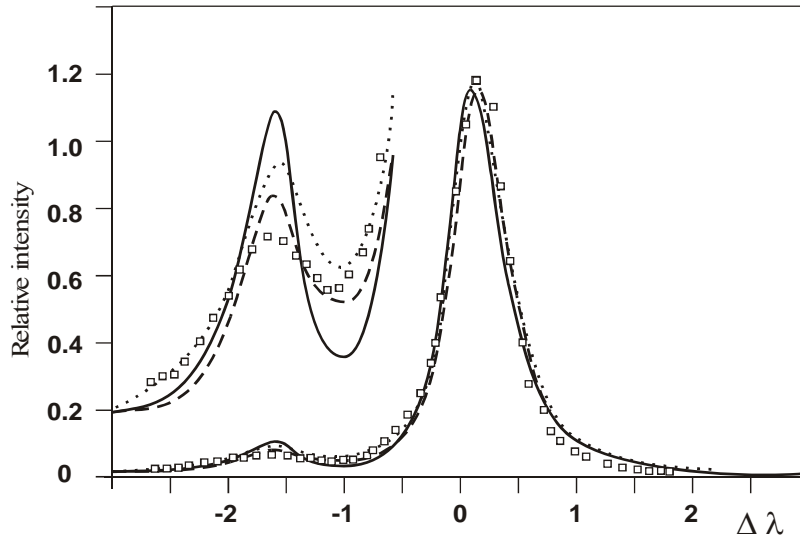


Fig. 5. Comparison of measured He I 447.1 nm line shape (squares) with theory: MMM (full), CC (dashed), and BCS (dotted line). Plasma parameters: $N_e = 1 \times 10^{15} \text{ cm}^{-3}$, $T_e = 18\,000 \text{ K}$, $T_g = 13\,000 \text{ K}$. Doppler and instrumental broadening included and all profiles are area normalized.

However, as illustrated in Fig. 5, the discrepancy of predicted forbidden line intensity with the experiment [20] still remains for all three theoretical approaches.

This is a main reason why experimentally determined formulas relating N_e with the parameters of helium lines with forbidden component such as F/A - forbidden (F) to allowed (A) line maximum intensity, D/A - deep (D) i.e. minimum intensity between forbidden and allowed line and A line intensity) and s - wavelength separation between F and A. determined by Czernichowski and Chapelle [21] are mainly used. Due to the fact that parameter s is not sensitive to distortion of the strong allowed line caused by the possible presence of a self-absorption effect, the following relation was used in this work

$$\log N_e [\text{m}^{-3}] = 23.056 + 1.586 \log (s[\text{nm}] - 0.156) + 0.225 [\log (s - 0.156)]^2 \quad (5)$$

where 0.156 nm in Eq.(6) is the separation between unperturbed F and A line.

The application of He I 447.2 nm line for determination of the medium electron densities was applied in the capillary discharge at $p=4$ mbar of gas mixture 1.5% CO_2 , 1.5% N_2 and He, see Figure 6. The capacitor of 0.36 μF charged up to the 6 kV was used to obtain peak current with duration of 3.6 μs .

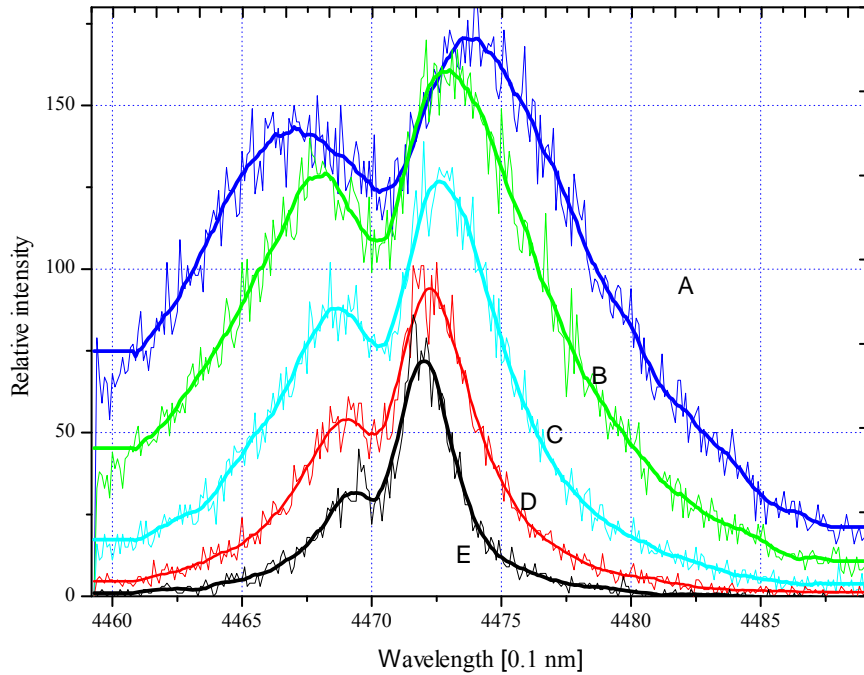


FIGURE 6. The shapes of the 447 nm line during plasma evaluation (A - 3.5; B - 4.5; C - 5.5; D - 6.5 and E - 7.5 μs after current maximum),

which corresponds to the $N_e = 3.4; 1.9; 1.2; 0.78$ and $0.35 \cdot 10^{16} \text{ cm}^{-3}$ respectively. The same procedure can be used for lower N_e determination, but with a use of a different amplification when recording forbidden or allowed component, as shown in Figure 7. It should be pointed out that great care must be taken when using He I lines with forbidden components for the determination of N_e lower than few times $10^{14} [\text{cm}^{-3}]$. At these densities, the low intensity of the forbidden component (less than few percents of the allowed one), may be masked by noise or in the presence of traces of nitrogen, molecular lines from 6-8 and 8-10 bands of the first negative system of N_2^+ .

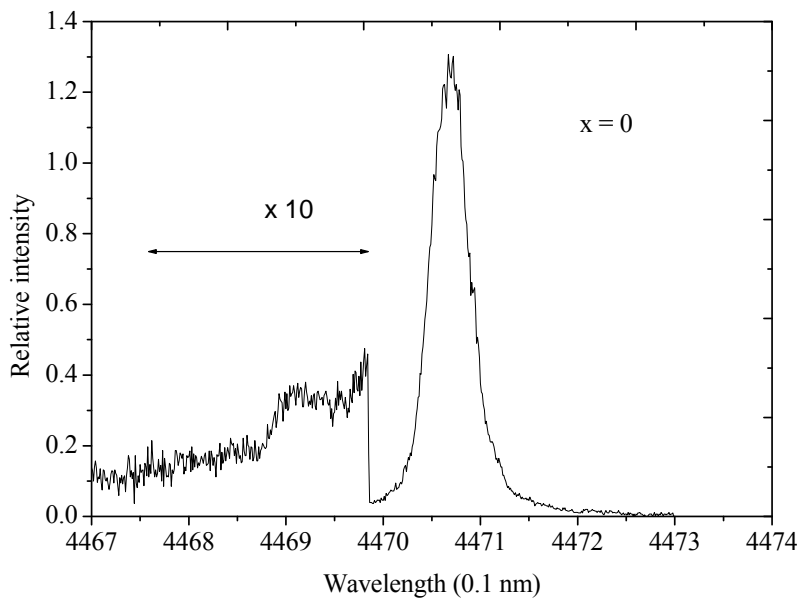


Fig. 7. Illustration of line shape recordings with different amplification of the photomultiplier signal. Line emitted from the center of the Mini MIP at height of 1mm from the torch orifice. The flow rate of He through the outer was 0.6 l/min, and He+ 3% H_2 through the inner capillary was 0.2 l/min.

3.3. Intensity of the N_2 and N_2^+ Molecular Band Heads

According to [22-24], the electron density in nitrogen and nitrogen/He plasmas can be determined from the intensity of N_2 second positive system (SPS) band head (0-0) at 337.1 nm ($C^3\Pi_u \rightarrow B^3\Pi_g$) and N_2^+ first negative system (FNS) band head of (0-0) at 391.4 nm ($B^2\Sigma_u^+ \rightarrow X^2\Sigma_g^+$).

Namely, by using the simplified kinetic model of the $N_2(C^3\Pi_u)$ state, see e.g. [23] and assuming that the steady-state population of the upper energy state is

equal zero, a linear relation between the 337.1 nm band intensity and the electron density at constant pressure and constant electric field may be obtained. This relation is confirmed with 5% accuracy in a volumetric near field microwave plasma [24].

A similar discussion can be applied to the band head of First Negative System of nitrogen ion ($B^2\Sigma_u^+ \rightarrow X^2\Sigma_g^+$) [23]. Due to an additional excitation process for the upper level population, the intensity of the 391.4 nm line has quadratic dependence upon electron density, i.e. $I_{(391.4 \text{ nm})} \sim N_u \sim A N_e^2 + B N_e$, where N_u is the population of the $B^2\Sigma_u^+$ state, while A and B are constants, which must be independently determined.

According to the authors [22], this method can be applied even in plasmas with non-Maxwellian electron energy distribution.

To apply the same method for N_e determination in other gas mixtures, N_2^+ ion fraction has to be calculated. The situation is more complex if Ar or H_2 are present in the gas mixture. The reactions $Ar^* + N_2 \rightarrow Ar + N_2^+$, $N_2^+ + H_2 \rightarrow N_2H^+ + H$ and $Ar^* + H_2 \rightarrow ArH^* + H$ and many others, have to be taken into account.

The band intensity method is tested in MIP at atmospheric pressure with power input of 100 W and at constant He flow rate of 0.7 l/min. The radial distributions of the band head intensities and hydrogen Balmer beta line shapes – H_β are obtained by Abel inversion procedure. From the determined H_β line shapes electron densities are calculated using approximate experimental formula, see Eq.2 in [5]. Finally, dependence of the molecular nitrogen band head intensities versus $\log N_e$ for different values of radius are presented in Figure 8.

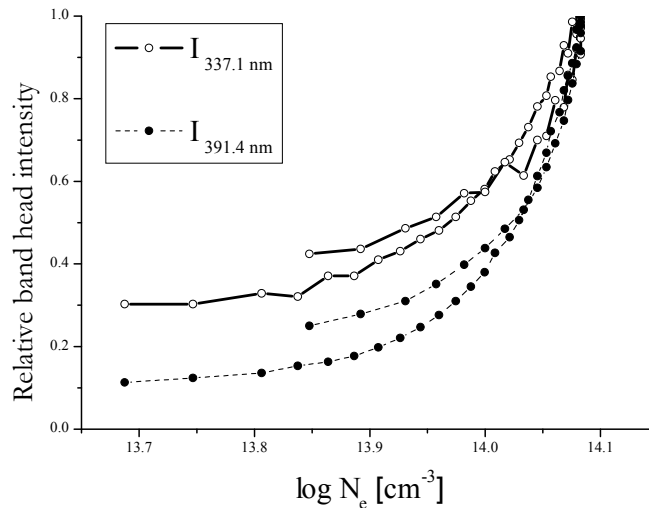


Fig. 8. Dependence of the molecular nitrogen band head intensities versus $\log N_e$ for different values of radius in MIP at atmospheric pressure Power input 100 W and flow rate of He 0.7 l/min.

It is evident that the application of this method for N_e determination requires further elaboration and experimental verifications in different plasma sources and gas mixtures. It should be noticed that the calibration of $\log N_2^+$ band intensity vs. $\log N_e$ determined using another independent diagnostic technique enables slope parameter determination. The extrapolation of intensity vs. N_e plot may be used for lower N_e plasma diagnostics.

4. CONCLUSIONS

At the end one can conclude that fitting of the neutral atom line profiles is useful for the medium electron density diagnostics, but a great precautions must be undertaken. This is especially important when more than one parameter fit of only one line without shift measurements is used for several plasma parameters determination.

The helium lines with forbidden components can be used in a very broad range of electron densities and even at lower than 10^{15} cm^{-3} . For lower densities the more complicated procedure must be used and further theoretical studies will be welcomed.

It should be stressed out that the molecular nitrogen band heads intensities offer a greatest possibility for diagnostics of very low densities, but a both theoretical and experimental studies in different plasma conditions are needed.

ACKNOWLEDGMENTS

This work is partially supported by the Ministry of Science and Environmental Protection of Serbia under projects 141032B.

REFERENCES

1. Q.Jin, Y.Duan, and J.A.Olivares, *Spectrochim.Acta* **B 52**, 131-161 (1997).
2. W.Locchte-Holtgreven, *Plasma Diagnostics*, American Institute of Physics, New York 1995.
3. J.Ropke, P.B.Davies, M.Kaning and B.P.Lavrov, Diagnostics of non-equilibrium molecular plasmas using emission and absorption spectroscopy, in "Low temperature plasma physics - Fundamental Aspects and Applications" Eds. R.Hippler, S.Pfau, M.Schmidt, K.H. Schonbach. Wiley-VCH, Berlin, N.Y. Toronto, 2001.
4. H.R.Griem, *Plasma Spectroscopy*, Academic Press, New York 1964.
5. M.Ivković, S.Jovičević and N.Konjević, *Spectrochimica Acta* **B 59**, 591-605, (2004).
6. S.Jovičević, M.Ivković, R.Zikic and N.Konjević, *J.Phys.B* **38**, 1249-1259 (2005).
7. M.Ivković Ben Nessib N and Konjević N, *J.Phys.B* **38**, 715-728 (2005).

8. S.Jovičević, M.Ivković, Z. Pavlovic, and N.Konjević, *Spectrochimica Acta* **B 55**, 1879-1893, (2000).
9. H.R.Griem, M.Baranger, A.C.Kolb and G.Oertel, *Phys.Rev.* **125**, 177 (1962).
10. Z. Mijatović, R.Kobilarov, B.T.Vujičić, D.Nikolić and N.Konjević, *J. Quant. Spectrosc.Radiat. Transfer* **50**, 329-335 (1993).
11. D.Nikolić, Z.Mijatović, S.Đurović, R.Kobilarov and N.Konjević, *J. Quant. Spectrosc.Radiat. Transfer* **70**, 67-74 (2001).
12. J.T.Davies and J.M.Vaughan, A new tabulation of the Voigt profile, *Astro-phys.J.* **137**, 1302-1305 (1963).
13. R.Kobilarov, N.Konjević, M.V.Popović, *Phys. Rev. A* **40**, 3871-3879 (1989).
14. Z.Mijatović, N.Konjević, M.Ivković, R.Kobilarov, *Phys. Rev.* **E51** 4891-4896 (1995).
15. N.Konjević, *Phys. Reports* **316**, 339-401 (1999).
16. T.D.Hahn and L.A.Woltz, *Phys.Rev.A* **42**, 1450 (1990).
17. D.Nikolić, S.Djurović, Z.Mijatović, R.Kobilarov and N. Konjević, in *Spectral Line Shapes*, International Conf. of Spectral Line Shapes, Pen State University Park, State College, Pensilvania USA, Vol 10, AIP Conf. Proc. **467**, New York AIP, 93, (1999).
18. V.Milosavljević and G.Poparić, *Phys.Rev.E* **63**, 036404 (2001).
19. V.Milosavljević, S.Djeniže and M.S.Dimitrijević, *Phys.Rev.E* **68**, 016402 (2003).
20. H. Richter and A.Piel, *J. Quant. Spectrosc.Radiat. Transfer* **33**, 615-626 (1985).
21. A.Czernichowski and J.Chapelle, *J. Quant. Spectrosc.Radiat. Transfer* **33**, 427-435 (1985).
22. K.Behringer and U.Fantz, *J.Phys.D: Appl. Phys.* **27**, 2128- 2135 (1994).
23. S.D.Popa, *J.Phys.D: Appl.Phys.* **29**, 416-418 (1996).
24. Exton R.J., Jeffrey Balla R., Hering G.C, Popovic S and Vuskovic L. *Proc. 34th AIAA Plasmadynamics and Lasers Conference*, 23-26 Jun 2003, Orlando, Florida, USA, paper 4181.